

Wave transformation at select locations along the Indian coast
through measurements, modelling and remote sensing

Thesis submitted for the Degree of

Doctor of Philosophy

in

Marine Sciences

to the

Goa University



by

Aboobacker V.M.

National Institute of Oceanography (CSIR)

Dona Paula, Goa – 403004, India.

November 2010

Dedicated to...

my "Uppa" and "Umma"

Statement

As required under the University Ordinance 0.19.8 (vi), I state that the present thesis entitled “**Wave transformation at select locations along the Indian coast through measurements, modelling and remote sensing**” is my original research work carried out at the National Institute of Oceanography, Goa and that no part thereof has been submitted for any other degree or diploma in any University or Institution.

The literature related to the problem investigated has been cited. Due acknowledgements have been made wherever facilities and suggestions have been availed of.

Aboobacker V.M.

National Institute of Oceanography
Dona Paula, Goa - 403 004

November 2010

Certificate

This is to certify that the thesis entitled “**Wave transformation at select locations along the Indian coast through measurements, modelling and remote sensing**” submitted by **Aboobacker V.M.** for the award of the degree of Doctor of Philosophy in the Department of Marine Sciences is based on his original studies carried out by him under my supervision. The thesis or any part thereof has not been previously submitted for any degree or diploma in any University or Institution.

Dr. P. Vethamony

National Institute of Oceanography
Dona Paula, Goa - 403004

Acknowledgments

It was a perfect decision, which I made during my visit to the National Institute of Oceanography (NIO) in December 2003 to meet Dr. P. Vethamony. In him, I found a 'Guide' and a person of good behaviour and positive approach. Since I joined in NIO as a Junior Research Fellow (JRF) during January 2004 under his supervision, he provided me a good platform to grow up in academic and personal level. He guided me with constant support and encouragement. He spent his valuable time with me for scientific discussions, which helped me to improve my understanding of ocean waves. It gives me great pleasure to thank him on this occasion, as I wind up the interpretations and discussions in the form of 'thesis'.

I am very grateful to the Council of Scientific and Industrial Research (CSIR), India for offering me research fellowships (JRF and SRF) to carry out research work of my interest.

I express my sincere gratitude to Dr. S.R. Shetye, Director, NIO, Goa, for providing me necessary facilities to carry out my work at NIO.

I thank Prof. H.B. Menon, Head, Department of Marine Sciences, Goa University for his valuable advice on several occasions, both scientific and administrative. I am thankful to the VC's nominee, Dr. S. Prasannakumar, Scientist, NIO, Goa, for providing critical comments and reviews on progress report.

I extend my sincere gratitude to Mr. K. Sudheesh, who helped me in learning modelling tools. Support from Mrs. Rashmi Vasuki in wave spectra analysis is greatly appreciated. Special thanks to Mr. Seemanth M., and Mrs. Dhanya Roshin for their help in setting up MM5 model. I acknowledge with gratitude, all those who participated in the field data collection, especially Mr. P.S. Pednekar and Mr. Ashok Kumar, K.

I thank Dr. Luigi Cavaleri, Former Director, Institute of Marine Science (ISMAR), Italy, for useful discussions on wave modelling, which helped me to improve the quality of the thesis. I thank Dr. M.T. Babu, Mr. S. Jayakumar, Dr. V. Sanil Kumar, Mr. D. Illangovan and Mr. R. Mani Murali for their support and encouragement during various stages of my research career.

My dearest friends, Grinson George, Vineesh, Divya Tenson, Sindhu Krishnakumar, Ricky, Ajay, Nisha Kurian, Deepthi Jagadeesh, Sini Anoop and Syam Sankar, who

always supported and encouraged me throughout my career. Their presence made me happier than ever. Thanks to all of them for their good words and deeds!

The pleasant ambience and nice work atmosphere in our lab is due to my dearest lab mates: Saheed, Renjith, Samiksha, Betty, Manu, Jyoti, Vinod, Suneel, Ratnamala and Mr. Krishnama Charyulu, who were very helpful and enthusiastic! I express my sincere gratitude to all of them.

It would be a difficult task to list all of my friends who supported directly or indirectly throughout my career! I extend my thanks to all those who helped me in various occasions. My special thanks to Mr. Simon, Mr. Vijayan, Dr. Yatheesh, Manoj Nambiar, Feby, Traicy, Prachi, Ratheesh, Smitha, Rupali, Siddharth, Vidya, Haris, Vijay, Laju, Ramya, Rajani, Nuncio, Ramesh, Sijin, Suprit and Manoj N.T for their support and encouragement.

All the success in my life is due to the everlasting support, love and prayers of my parents! May Allah bless them with good health, happiness and prosperity! I extend my thanks to my parents, all my family members and friends from my native, who were ever supportive and very kind in every situation in my life. At last, but not the least, love and regards to my (niece) sweet Hifa mol .

Aboobacker V.M.

National Institute of Oceanography, Goa

November 2010

Abstract

Wind generated wave is the dominant forcing parameter for most of the nearshore processes. Accurate and fine resolution (both spatial and temporal resolutions) wave information is very essential for navigation, design of coastal/offshore structures and other marine activities. When waves generated by storms leave the zone of generation, they couple with locally generated waves, and create complex characteristics in the nearshore region. In the past, the source of wave information was mainly from ship observations. Advanced technologies led to the development of directional wave rider buoys and moored buoys which measure directional wave energy spectra at fixed point locations. Remote sensing sensors such as altimeter and scatterometer provide wind speed & wave height and wind speed & direction, respectively covering a large space. At times, in situ point measurements as well as satellite observations may not be adequate for site specific studies such as coastal development and beach stability. In this context, numerical modelling provides an opportunity to obtain the required wave information in fine resolution. Wave modelling results are also crucial to support forecasts and warnings to reduce risk of accidents and improve the efficiency of marine operations.

Wave characteristics along the Indian coast have been studied by earlier researchers based on ship observations, buoy measurements and remote sensing data. Most of these studies are restricted to specific locations or periods. However, a complete description of sea states for all seasons and extreme events is still in demand. Further, interaction between multi-directional and multi-frequency waves (both swells and wind seas) is still recognized as a complex phenomenon in the coastal region, as the local wind seas play a major role in controlling the wave generation and propagation mechanisms in this region. Influence of sea breeze on wind sea generation along the west coast of India is dominant during pre-monsoon season. The superimposition of these wind seas with pre-existing swells results in complex sea states, which makes the sea-faring more difficult than a single wave system. Generation and propagation of the multi-directional swells in the Arabian Sea, especially during pre-monsoon and NE monsoon seasons, their interaction with local wind seas along the west coast of India and their transformation at nearshore regions are a few scientific problems which find applications in the areas mentioned elsewhere. In this background, objectives of the present study are framed as follows:

- i) understanding the wave generation and propagation processes in the select nearshore regions along the Indian coast through measured data
-

- ii) validation of wave modelling results of deep and shallow waters using measurements and remote sensing data
- iii) to study the interaction between pre-existing swells and wind seas generated by coastal winds
- iv) prediction of wave transformation along the select Indian coasts using high resolution winds such as MM5

Chapter 1: Introduction, describes wind waves in general, regional wave scenarios, objectives, area of study and literature review.

Chapter 2: Data and methodology, describes the data used (wind, wave and pressure) and the methodologies applied. Wave measurements carried out at several deep and shallow waters locations in the north Indian Ocean using moored data buoys, directional wave rider buoys and non-directional wave recorders have been used in the present study along with satellite data (Jason-1). Winds measured using Autonomous Weather Station (AWS) and moored data buoys, QuikSCAT winds, re-analysed winds from various sources such as NCEP (National Centers for Environmental Prediction, USA), IFREREMER (French Research Institute for Exploitation of the Sea) and NCMRWF (National Centre for Medium Range Weather Forecasting, India), and MM5 (Mesoscale Model) were analysed and used in the wave model. Cyclone track data obtained from JTWC (Joint Typhoon Warning Centre, U.S.A.) and pressure data obtained from IDWR were also analysed. Wave spectra were separated into wind sea and swell energies and the corresponding wave parameters were calculated using the methodology provided by Gilhousen and Hervey (2001). The wind sea and swell parameters were further analysed to study their characteristics during different seasons. The dominance (in percentage) of swells and wind seas has been computed and analysed for studying the monthly, seasonal and annual variations. Validation of MM5 winds and details of numerical models used are also described in Chapter 2.

Chapter 3: Numerical simulations - model set up and validation, it explains the setting up of numerical model for the Indian Ocean, model calibration and validation of model results with in situ and remote sensing data. Regional and local model domains were setup for the Indian Ocean (65° S to 30° N and 20° E to 130° E) and select coastal regions (Dwarka, Ratnagiri, Goa, Paradip and Dhamra). Bathymetry is set for rectangular grids and flexible

mesh. Moreover, a model with varying resolutions at deep water (coarse mesh) and coastal regions (fine mesh) has been setup to study the nearshore wave transformation along the Indian coast. Wind data from various sources have been applied as input parameter to simulate waves in the Indian Ocean. Sensitivity to various wind fields has been tested. Wind seas off Goa have been simulated using MM5 winds, and validated with calculated (separated from measured spectra) wind sea parameters.

Chapter 4: Seasonal response of coastal waves along the Indian coast: spectral approach. This chapter describes wave characteristics during monsoons and extreme events, dominance of swells along the west coast of India, potential swell generation regions, “Shamal” swells in the Arabian Sea and superimposition of coastal wind seas on pre-existing swells. The wave energy spectra off typical east coast (off Paradip) and west coast (off Goa) of India show the response of coastal waves to the seasons. It has been found that the spectra during extreme events are primarily single-peaked, and multi-peaked spectra of other seasons indicate the presence of multi-directional wave systems. The analysis of dominance of swells and wind seas show that the swells are dominated along the Indian coast during major part of the years and wind seas are dominated along the west coast of India during the pre-monsoon season. Potential swell regions were identified from measurements and modelling results and their propagation towards the west coast of India has been analysed. The presence of “Shamal” swells has been identified from the measured waves along the west coast of India during winter season. Typical mean periods of the Shamal swells are between 6 and 8 s and significant wave heights are between 1.0 and 2.0 m along the west coast of India. The generation and propagation of these “Shamal” swells and their influence along the west coast of India have been studied using numerical simulations. The results are discussed in detail.

The wind and wave data off Goa during pre-monsoon season (May 2005) reveals a distinct and systematic diurnal variation in wind speed, wave height and wave period, especially increase in wave height and decrease in wave period with increase in the intensity of coastal winds due to sea breeze system. Measured wave spectra distinctly bring out salient features of deep water swell and wind seas generated by the local sea breeze. Numerical simulations reproduced the characteristics of this daily cycle. The characteristic features observed in the wave parameters are due to the superimposition of wind seas with pre-existing swells. This phenomenon has been subject to detailed analysis, and the results are discussed in Chapter 4.

Chapter 5: Wave transformation along open coasts and semi-enclosed regions. This study illustrates the nature of wave transformation that can occur along the Indian coast. Wave patterns along the west coast of India are nearly the same, but wave heights are in the increasing order of magnitude from south to north. Wave heights along the east coast of India are in the increasing order during pre-monsoon and SW monsoon seasons, and in the decreasing order during NE monsoon season, from south to north, and the reduction among various depths are relatively less as compared to those along the west coast of India. Towards application of wave modelling, a case study has been carried out for the Mormugao Port region (Goa) to demarcate the inland vessels' limit (IVL) based the distribution of significant wave heights. Results are discussed in detail.

Chapter 6: Summary and conclusions. It describes the summary of the entire work and the main conclusions of the present study. Scope is provided for future work.

Contents

Statement	iii
Certificate	iv
Acknowledgments	v
Abstract	vii
List of Tables	xv
List of Figures	xvii
Chapter 1 Introduction	1 - 26
1.1 Ocean surface waves	1
1.1.1 Definitions and relations	1
1.1.2 Wave generation, growth and decay	3
1.2 Regional wave scenarios	5
1.3 Objectives	7
1.4 Area of study	7
1.5 Literature review	11
1.5.1 Wave generation and growth – historical perspective	11
1.5.2 Wave energy spectrum	14
1.5.3 Remote sensing	16
1.5.4 First, second and third generation models	17
1.5.4.1 First generation models	18
1.5.4.2 Second generation models	19
1.5.4.3 Third generation models	20
1.5.5 Impact of sea breeze on nearshore waves	22
1.5.6 Wave transformation	23
1.6 Studies along the Indian Ocean region	24
Chapter 2 Data and methodology	27 - 47
2.1 Introduction	27
2.2 Data used	28
2.2.1 Directional wave rider buoy	28
2.2.2 Moored buoys	32

2.2.3	Non-directional wave recorder	32
2.2.4	Autonomous Weather Station (AWS)	34
2.2.5	NCEP re-analysis winds	34
2.2.6	IFREMER/CERSAT Blended winds	35
2.2.7	NCMRWF winds	35
2.2.8	QuikSCAT winds	36
2.2.9	MM5 winds	36
2.2.10	Jason-1 Altimeter	36
2.2.11	JTWC and IDWR	37
2.2.12	Comparison of analysed winds with measured winds	38
2.3	Methodology	41
2.3.1	Separation of wind sea and swell	41
2.3.2	Validation of MM5 winds	43
2.3.3	Wave modelling	45
2.3.3.1	MIKE 21 OSW	45
2.3.3.2	MIKE 21 NSW	46
2.3.3.3	MIKE 21 SW	47
Chapter 3	Numerical simulations: model setup and validation	48 - 75
3.1	Introduction	48
3.2	Model setup	48
3.2.1	Model domain and bathymetry	48
3.2.2	Basic formulations	54
3.2.3	Input parameters	56
3.2.4	Energy transfer	57
3.2.5	Calibration parameters	57
3.2.5.1	White capping	57
3.2.5.2	Bottom friction	57
3.2.5.3	Wave breaking	58
3.2.6	Initial conditions	58
3.2.7	Boundary conditions	58
3.2.8	Output parameters	59

3.3	Model validation	61
3.3.1	Validation at deep water locations	61
3.3.2	Validation at nearshore regions	64
3.3.3	Sensitivity test	70
3.4	Simulations using MM5 winds	71

**Chapter 4 Seasonal response of coastal waves along the Indian coast:
spectral approach 76 - 125**

4.1	Introduction	76
4.2	Wave characteristics during monsoons and extreme events	76
4.2.1	Along the east coast of India	76
4.2.2	Along the west coast of India	83
4.3	Dominance of swells along the west coast of India	88
4.4	Potential swell generation regions	96
4.4.1	Wave observations	97
4.4.2	Numerical model results	98
4.5	“Shamal” swells in the Arabian Sea	101
4.5.1	Introduction	101
4.5.2	Characteristics of “Shamal” swells	102
4.5.3	Generation and propagation	107
4.5.4	Influence along the west coast of India	109
4.6	Superimposition of coastal wind seas on pre-existing swells	111
4.6.1	Sea breeze along the west coast	112
4.6.2	Diurnal variations in the nearshore waves	116

**Chapter 5 Wave transformation along open coasts and semi-enclosed
regions 126 - 161**

5.1	Introduction	126
5.2	Wave transformation along open coasts	126
5.2.1	Deep water waves from Jason-1	126
5.2.2	Waves at nearshore regions	128
5.2.2.1	Measurements	128
5.2.2.2	Modelling results	132

Contents	xiv	
5.3	Wave transformation at semi-enclosed regions	143
5.3.1	Dhamra Port – naturally protected area	143
5.3.2	Mormugao Port – artificially protected area	148
5.4	Inland vessel’s limit off Mormugao Port – a case study	154
5.4.1	Introduction	154
5.4.2	Data and methods	154
5.4.3	Results and discussion	155
Chapter 6	Summary and conclusions	162 - 168
6.1	Summary	162
6.2	Conclusions	166
6.3	Future prospects	168
References		169 – 183
Annexure I: Published papers		
Annexure II: List of papers under revision		

List of Tables

	Page
Table 2-1. Details of wave measurement locations, water depth, measurement duration and data interval (directional wave rider buoys).	31
Table 2-2. Details of wave measurement locations, water depth, measurement duration and data interval (NIOT moored buoys).	33
Table 2-3. Details of wave measurement locations, water depth, measurement duration and data interval (non-directional wave recorder).	33
Table 2-4. Details of AWS wind measurement locations, measurement height, measurement duration and data interval.	34
Table 2-5. Correlation coefficient, bias and r.m.s. error between measured and simulated winds off Goa (May 2005).	44
Table 3-1. Integral wave parameters obtained from wave simulations.	60
Table 3-2. Statistical parameters estimated between measured and modelled wave parameters at DS1.	63
Table 3-3. Statistical parameters estimated between Jason-1 and model significant wave heights at G1 and P1.	63
Table 3-4. Statistical parameters estimated between measured and model wave parameters at B1 (off Goa) and B8 (off Paradip).	67
Table 3-5. Statistical parameters estimated between measured and modelled (using NCEP, Blended and QuikScat winds) wave parameters at B2.	71
Table 3-6. Statistical parameters estimated between measured and modelled wind sea parameters at B2 and B3.	72
Table 4-1. Monthly variations of H_s and T_m for the swell and sea.	85
Table 4-2. Monthly percentage dominance of swell and sea.	90
Table 5-1. Mean H_s and % reduction at various measurement locations along the west coast of India.	132
Table 5-2. Seasonal and annual mean and standard deviation of significant wave heights at various depths off Mumbai, Goa and Kochi.	137
Table 5-3. Seasonal and annual mean and standard deviation of significant wave heights at various depths off Nagappattinam, Visakapattinam and Paradip.	141
Table 5-4. Maximum, mean and standard deviation of significant wave heights during 2005 in the vicinity of Dhamra Port.	148
Table 5-5. Maximum, mean and standard deviation of significant wave heights during February 1996 – May 1997 in the vicinity of Mormugao Port.	153
Table 5-6. Monthly variations in the significant wave height and mean wave period off Goa during February 1996 - May 1997.	157

Table 5-7.	Statistics of significant wave heights exceeding 2.0 m during SW monsoon season	159
Table 5-8.	Range of significant wave height derived from available moored buoy data off Goa.	159

.

List of Figures

	Page
Figure 1-1. Classification of ocean waves by wave period (Munk, 1951).	1
Figure 1-2. A simple sinusoidal wave (WMO, 1998).	2
Figure 1-3. Indian Ocean (top) and Indian coastal regions (bottom) considered for the study.	9
Figure 1-4. (a) Mormugao Port region including the locations of wave rider buoys and moored data buoy off Goa and (b) breakwaters in the Mormugao Port.	10
Figure 1-5. Dhamra Port and surrounding areas.	11
Figure 2-1. Datawell wave rider buoy and associated parts.	29
Figure 2-2. Wave measurement locations using wave rider buoys (B1 to B10), moored buoys (DS1 and SW3) and non-directional wave recorder (N1).	30
Figure 2-3. Jason-1 data extraction locations off Goa and Paradip.	37
Figure 2-4. Comparison between measured (buoy) and analysed (NCEP, Blended and QuikSCAT) winds: (a) wind speed and (b) wind direction.	39
Figure 2-5. Scatter between measured wind speed and: (a) NCEP, (b) Blended and (c) QuikSCAT wind speeds.	40
Figure 2-6. Comparison between measured and NCMRWF wind speed and direction.	41
Figure 2-7. Comparison of separation frequencies obtained from ‘Gilhousen and Harvey’ and ‘Wang and Hwang’ methods.	43
Figure 2-8. Comparison between measured and modelled wind vectors at Dona Paula coastal station (May 2005).	45
Figure 3-1. Model domain, bathymetry and flexible mesh used for wave simulations in the Indian Ocean.	49
Figure 3-2. Model domain and bathymetry used for OSW simulations in the Indian Ocean.	50
Figure 3-3. Domain, bathymetry and flexible mesh used for the local model (SW) simulations along the west coast of India: (a) off Goa, (b) off Ratnagiri and (c) off Dwarka.	51
Figure 3-4. Domain, bathymetry and flexible mesh used for the local model (SW) simulations along the east coast of India: (a) off Paradip, (b) off Dhamra.	52
Figure 3-5. Domain and bathymetry used for the NSW simulations off Goa.	53
Figure 3-6. Bathymetry and flexible mesh used for SW simulations for wave transformation along the Indian coast.	54

Figure 3-7.	Comparison between measured and modelled wave parameters at DS1: (a) significant wave height and (b) mean wave period.	62
Figure 3-8.	Scatter between measured and modelled H_s and T_m at DS1.	63
Figure 3-9.	Comparison between Jason-1 and modelled H_s off: (a) Goa (at G1) and (b) Paradip (at P1).	64
Figure 3-10.	Scatter between Jason-1 and modelled H_s at G1 (off Goa) and P1 (off Paradip).	64
Figure 3-11.	Comparison between measured and modelled wave parameters at B1 (off Goa): (a) significant wave height, (b) mean wave period and (c) mean wave direction.	65
Figure 3-12.	Comparison between measured and modelled wave parameters at B8 (off Paradip): (a) significant wave height, (b) mean wave period and (c) mean wave direction.	66
Figure 3-13.	Scatter between measured and modelled wave parameters at B1 (off Goa): (a) resultant H_s , (b) resultant T_m , (c) swell H_s , (d) swell T_m , (e) wind H_s sea and (f) wind sea T_m .	68
Figure 3-14.	Scatter between measured and modelled wave parameters at B8 (off Paradip): (a) resultant H_s , (b) resultant T_m , (c) swell H_s , (d) swell T_m , (e) wind sea H_s and (f) wind sea T_m .	69
Figure 3-15.	Comparison between measured and modelled wind sea parameters at B2: (a) significant wave height, (b) mean wave period and (c) mean wave direction.	73
Figure 3-16.	Comparison between measured and modelled wind sea parameters at B3: (a) significant wave height, (b) mean wave period and (c) mean wave direction.	74
Figure 3-17.	Scatter between measured and modelled (a) wind sea H_s and (b) wind sea T_m at B2.	75
Figure 3-18.	Scatter between measured and modelled (a) wind sea H_s and (b) wind sea T_m at B3.	75
Figure 4-1.	Pressure levels during May 1996–December 1996.	77
Figure 4-2.	Significant wave height pattern during an extreme event (23 May – 02 June, 1996) indicating wave growth and decay.	78
Figure 4-3.	Typical wave spectra during (a) 26 July at 09 h, (b) 3 Aug 1996 at 09 h and (c) 3 July 09 h.	80
Figure 4-4.	Measured directional energy spectra from 00 h to 21 h (for every 3 h) on 26 July 1996.	80
Figure 4-5.	Measured directional energy spectra from 00 h to 21 h (for every 3 h) on 15 November 1996.	81

Figure 4-6.	Modelled directional energy spectra on 26 July for every 3 h simulations (from 00 h to 21 h).	82
Figure 4-7.	Distribution of (a) significant wave height, (b) mean wave period and (c) mean wave direction for the resultant wave, swell and wind sea during February 1996 to May 1997.	84
Figure 4-8.	Typical directional wave energy spectra and wind rose during (a) pre-monsoon, (b) SW monsoon and (c) NE monsoon seasons.	86
Figure 4-9.	Swell patterns during a tropical storm in the Arabian Sea.	88
Figure 4-10.	Scatter diagrams of resultant H_s vs. swell H_s and resultant H_s vs. wind sea H_s during (a) pre-monsoon, (b) SW monsoon and (c) NE monsoon seasons.	93
Figure 4-11.	(a) Locations of NCEP wind extracted and (b) wind speed and direction at W1 (off Goa) during Feb 1996 to May 1997.	94
Figure 4-12.	Scatter diagrams (a) wind speed vs. wind sea H_s and (b) wind direction vs. wind sea direction.	95
Figure 4-13.	Scatter diagram of significant wave heights showing the dominance of wind sea and swell during (a) pre-monsoon, (b) SW monsoon and (c) NE monsoon seasons.	95
Figure 4-14.	Typical swell patterns in the Arabian Sea during (a) pre-monsoon season (12 April 1997) and (b) NE monsoon season (10 December 1996).	96
Figure 4-15.	Significant wave heights off Kochi, Mangalore, Goa, Ratnagiri and Mumbai during (a) pre-monsoon, (b) SW monsoon and (c) NE monsoon seasons.	100
Figure 4-16.	Study area and measurement locations.	102
Figure 4-17.	Measured wave and wind parameters off Ratnagiri; (a) significant wave height, (b) mean wave period, (c) mean wave direction and (d) AWS wind speed and direction.	104
Figure 4-18.	Typical directional energy spectra during (a) Shamal period and (b) non-Shamal period.	105
Figure 4-19.	Typical wind vectors over the Arabian Sea associated with (a) NE monsoon and (b) Shamal event.	106
Figure 4-20.	Significant wave height vectors in the Arabian Sea during 02-04 Feb 2008 representing the generation and propagation of Shamal swells.	108
Figure 4-21.	Significant swell heights off Kochi, Mangalore, Goa, Ratnagiri and Mumbai at 25 m water depth, extracted from the simulation results.	109
Figure 4-22.	Measured wave parameters off Dwarka at B6 during 05 Dec 2007 – 05 Jan 2008: (a) significant wave height, (b) mean wave period and (c) mean wave direction.	110

Figure 4-23.	Measured wave parameters off Goa at B1 during January 1997: (a) significant wave height, (b) mean wave period and (c) mean wave direction.	111
Figure 4-24.	AWS wind distribution at Dona Paula during 12 May 2005.	113
Figure 4-25.	QuikSCAT winds off Goa: (a) locations from offshore to coast (Q1 to Q5) and (b) wind speed distribution at the locations Q1 to Q5.	114
Figure 4-26.	Typical wind vectors (CERSAT/IFREMER blended winds) in and around Goa region during 05 May 2005.	115
Figure 4-27.	Typical wind vectors on a daily cycle during pre-monsoon season, as simulated in MM5.	116
Figure 4-28.	(a) AWS wind distribution at Dona Paula and (b) significant wave height and mean wave period at B2 during 12 May 2005.	117
Figure 4-29.	Distribution of (a) AWS winds at Dona Paula coastal station, (b) Significant wave height at B2 and B3 and (c) Mean wave period at B2 and B3.	119
Figure 4-30.	Directional energy spectra during 00h to 21h (for every 3 hour) on 19 May 2005.	120
Figure 4-31.	Typical 1D spectra during May 2005.	120
Figure 4-32.	Measured significant wave height and mean wave period during May 2005 at B2, showing an inverse proportion among their variations.	121
Figure 4-33.	Significant wave heights during 1-21 May 2005 : (i) Jason-1 (1 degree x 1 degree grid resolution) extracted at 15 ⁰ N, 73 ⁰ E on an alternate 3 and 4 days average, (ii) Measured at B2 (iii) Modelled data extracted at B2.	121
Figure 4-34.	Scatter between measured and modelled significant wave heights.	122
Figure 4-35.	Typical wind sea H_s vectors during sea breeze dominated period, simulated using MM5 winds.	123
Figure 4-36.	Measured and modelled significant wave height and mean wave period at location B2.	124
Figure 4-37.	Typical H_s vectors during sea breeze dominated period.	125
Figure 5-1.	Jason-1 significant wave height distribution during 2005: (a) off Goa and (b) off Paradip.	127
Figure 5-2.	Measurement locations and bathymetry contours off Goa, Ratnagiri and Dwarka.	130
Figure 5-3.	Significant wave heights measured at nearshore depths off: (a) Goa, (b) Ratnagiri and (c) Dwarka.	131
Figure 5-4.	Significant wave heights at various water depths off Mumbai, Goa and Kochi during 2005.	135

Figure 5-5.	Diurnal variations in significant wave heights at various water depths off Mumbai, Goa and Kochi during pre-monsoon season (May 2005).	136
Figure 5-6.	Mean H_s at various depths ranging from 100 to 5 m during pre-monsoon, SW monsoon and NE monsoon seasons off: (a) Mumbai, (b) Goa and (c) Kochi.	138
Figure 5-7.	Significant wave heights at various water depths off Nagappattinam, Visakhapatnam and Paradip during 2005.	139
Figure 5-8.	Significant wave heights at various water depths off Nagappattinam, Visakhapatnam and Paradip during pre-monsoon season (May 2005).	140
Figure 5-9.	Mean H_s at various depths ranging from 100 to 5 m during pre-monsoon, SW monsoon and NE monsoon seasons off: (a) Nagappattinam, (b) Visakapattinam and (c) Paradip.	142
Figure 5-10.	Flexible mesh and bathymetry close to the Dhamra region.	145
Figure 5-11.	Comparison between measured and modelled wave parameters at location B10: (a) significant wave height, (b) mean wave period and (c) mean wave direction.	146
Figure 5-12.	Comparison between measured and modelled (a) significant wave height and (b) mean wave period off Dhamra (at C1).	147
Figure 5-12.	(a) Significant wave height and (b) mean wave direction, at locations B10, O1 and C1 during 2005.	148
Figure 5-14.	(a) Model domain and flexible mesh selected for the wave transformation simulations off Goa and (b) Flexible mesh and bathymetry close to the Port and extraction locations - outside breakwater (OP) and inside breakwater (IP1 and IP2).	151
Figure 5-15.	Comparison between measured and modelled wave parameters at location B3.	152
Figure 5-16.	Significant wave height and mean wave direction obtained at locations OP, IP1 and IP2 during Feb 1996 – May 1997.	153
Figure 5-17.	Typical wave spectra at 2 locations off Goa during 13 May 2005 (00 h, 03 h, 06 h, 09 h, 12 h, 15 h, 18 h, 23 and 21 h respectively).	158
Figure 5-18.	Typical significant wave height distribution off Mormugao Port during SW monsoon.	160
Figure 5-19.	IVL regions demarcated based on wave heights (April 2005) with existing smooth and partially smooth waterlines.	161

Chapter 1
Introduction

Chapter 1

Introduction

1.1. Ocean surface waves

Ocean surface waves are generated due to various forces acting on the ocean. The characteristics of the waves depend on controlling forces such as wind stress, earthquakes, gravity, Coriolis force and surface tension. Tidal waves are generated by the response to gravity of the moon and the sun, and are rather large-scale waves. Capillary waves, at the other end of the scale, are generated by surface tension in the water. For gravity waves, the major determining factors are earth's gravity and buoyancy of water (WMO, 1998). Based on period, the time taken by successive wave crests to pass a fixed point, the waves are classified into different categories. Figure 1- 1 shows their classifications by wave period (Munk, 1951). Waves with period less than 0.1 s are called capillary waves, between 0.1 and 1 s are gravity-capillary waves and between 1 and 30 s are ordinary gravity waves. The long-period waves such as storm surges and tsunamis have a range of period between 5 min. and 12 h, whereas the tidal waves range between 12 h and 24 h. Gravity waves generated by winds are present on the sea surface.

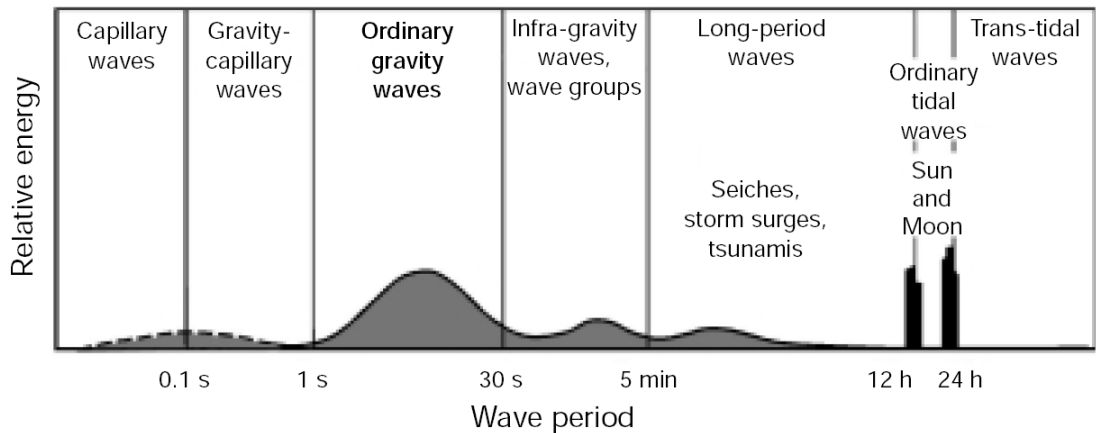


Figure 1- 1. Classification of ocean waves by wave period (Munk, 1951).

1.1.1. Definitions and relations

The simple wave motion is represented by a sinusoidal, long-crested and progressive wave (Figure 1- 2). The horizontal distance between two successive crests or troughs is called the

wavelength represented by λ , the time interval between the passage of successive crests or troughs passed a fixed point is called the *wave period* represented by T . The magnitude of the maximum displacement from mean sea-level is called the *wave amplitude* represented by a and the difference in surface elevation between the wave crest and the previous wave trough is called the *wave height* represented by H . For a simple sinusoidal wave $H = 2a$. The *frequency*, f , is the number of crests which pass a fixed point in 1 s; unit is Hertz and is same as $1/T$. The *phase speed*, c , is the speed at which the wave profile travels, i.e. the speed at which the crest and trough of the wave advance. The *wave steepness* is the ratio of wave height to wave length (H/λ).

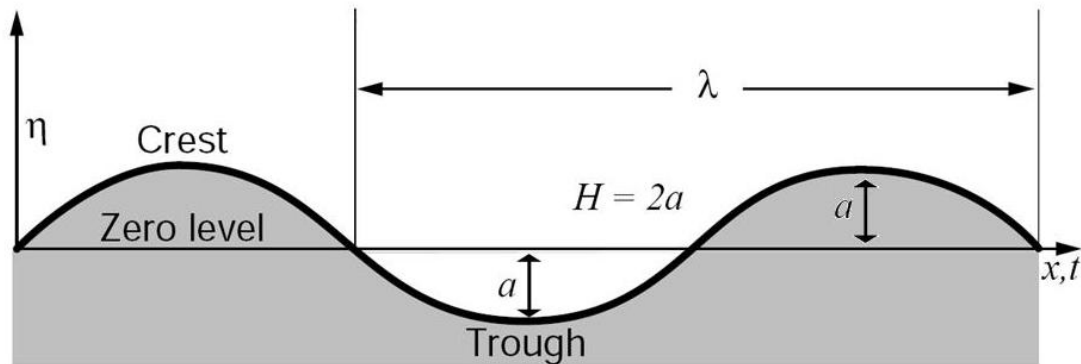


Figure 1- 2. A simple sinusoidal wave (WMO, 1998).

The wave profile has the form of a sinusoidal wave:

$$\eta(x, t) = a \sin(kx - \omega t) \quad (1.1)$$

where, η is the surface elevation, $k = 2\pi/\lambda$ is the *wavenumber* and $\omega = 2\pi/T$, the *angular frequency*. Wavenumber is a cyclic measure of the number of crests per unit distance and angular frequency is the number of radians per second. The variation of wave speed with wavelength is called *dispersion*, and the functional relationship is called the *dispersion relation*. The dispersion relation follows from the equations of motion for finite water depth can be expressed in terms of frequency, wavelength and water depth as follows:

$$\omega^2 = gk \tanh(kh) \quad (1.2)$$

where, g is gravitational acceleration and h is the water depth. In deep water ($h > \lambda/4$), $\tanh kh$ approaches unity. Hence,

$$\omega^2 = gk \quad (1.3)$$

Therefore, wave speed in deep water is:

$$c = \lambda/T = \omega/k = \sqrt{g/k} \quad (1.4)$$

When the relative water depth becomes shallow ($h < \lambda/25$), $\tanh(kh)$ approximately equals kh . Hence, Equation 1.2 becomes,

$$\omega^2 = gk^2h \quad (1.5)$$

Therefore, wave speed in shallow water is:

$$c = \sqrt{gh} \quad (1.6)$$

Hence, the waves in the shallow water are non-dispersive as the wave speed is independent of k .

1.1.2. Wave generation, growth and decay

The main input of energy to the ocean surface comes from the wind. Transfer of energy to the wave field is achieved through the surface stress applied by the wind and this varies as the square of the wind speed. Wind wave generation and growth are mainly controlled by three factors; wind speed, duration and fetch. Fetch is the area where the wind blows continuously without change in direction. Strong winds with long duration over a wide fetch could generate larger waves with long periods. These waves can travel hundreds (or thousands) of kilometers without much dissipation until it feels the bottom. In deep waters, the particle motion associated with the waves is circular and it is negligible beyond a depth equals $\lambda/2$. In shallow waters, the particle motion is elliptical and this extends upto the bottom.

Two mechanisms associated with wind wave growth are Philips' resonance (Philips, 1957) and shear flow instability (Miles, 1957). The resonance theory explains that small pressure fluctuations associated with turbulence in the airflow above the water are sufficient to induce small perturbations on the sea surface and to support a subsequent linear growth as the wavelets move in resonance with the pressure fluctuations. The theory of shear flow instability explains that air flow sucking at the crests and pushing on the troughs enables the waves to grow and the growth is exponential.

The ocean surface is represented by a combination of irregular wave components with different wavelength, amplitude and direction. Its chaotic pattern is due to the sum of wave components present at the region. The superimposition of various wave components creates an irregular pattern, which is usually observed at the wave generating areas. The waves in the generating area are termed as ‘wind seas’. The waves propagating out from the generating area attain near sinusoidal and orderly patterns, and are termed as ‘swells’. Total energy associated with the waves is equally divided between kinetic energy and potential energy. The energy moves with the speed of group of waves rather than individual waves. The speed associated with each individual waves is called ‘phase speed’ and the velocity associated with the wave groups or the velocity with which the energy is propagated is called ‘group velocity’. In deep water, the magnitude of the group velocity (c_g) is half the phase speed (c), and, in shallow water, the group velocity is same as the phase velocity. The general expression for group velocity (c_g) in finite water depth (h) is given by,

$$c_g = \frac{c}{2} \left(1 + \frac{2kh}{\sinh 2kh}\right) \quad (1.7)$$

Wave energy dissipation occurs mainly due to three processes; whitecapping, wave-bottom interaction and surf breaking. As waves grow, the steepness increases until it reaches a critical point, where the waves break. Whitecapping is highly non-linear and it limits the wave growth. ‘Shoaling’ is the effect of sea bottom when waves propagate into shallow water without changing direction. Generally, this enhances wave height and is best demonstrated when wave crests are parallel to depth contours. When waves enter into transitional depths, if they are not travelling perpendicular to the depth contours, the part of the wave in deeper water moves faster than the part in shallower water, causing the crest to turn parallel to the bottom contours. This phenomenon is called ‘refraction’. Refraction causes reduction in wave energy, which depends on the depth contours and bottom characteristics. Obstruction, such as breakwaters, causes the energy to be transformed along a wave crest at the lee of the obstruction. This is called ‘diffraction’ and it causes much reduction in the wave height. Surf breaking occurs at extremely shallow waters, where depth and wave height are of the same order of magnitude (Battjes and Janssen, 1978).

1.2. Regional wave scenarios

Waves generated by winds or storms become ocean swells when they leave their generation zone, and travel long distances across the globe. Empirical data supports the idea that wind seas and swells together account for more than half of the energy carried by all waves on the ocean surface, surpassing the contribution of tides, tsunamis, coastal surges, etc. (Kinsman, 1965). Investigations on the contribution of ocean swell to the wind wave climate are, therefore, of great importance in a wide range of oceanographic studies, coastal management activities and ocean engineering applications. Design of coastal structures to a large extent depends on waves than any other environmental factors. When swells couple with locally generated waves, create complex wave characteristics in the nearshore region. The coexistence of wind sea and swell can significantly affect sea-keeping safety, offshore structural design, small boat operations and ship passages over harbour entrance and surf forecasting (Earle 1984). It also affects the dynamics of near-surface processes such as air-sea momentum transfer (Dobson et al., 1994; Donelan et al., 1997; Hanson and Phillips, 1999; Mitsuyasu, 2002). A wide range of activities such as shipping, fishing, recreation, coastal and offshore industry, coastal management and pollution control are affected by the wind waves (WMO, 1998).

In the past, the only source of wave information was visual observations made from ships. Advance technologies led to the development of directional wave rider buoys and moored buoys which measure the directional wave energy spectra. In situ wave measurements are essential for deriving design wave parameters and validation of wave model results. Remote sensing technologies have made good progress in the collection of various ocean parameters, including waves - altimeters and SAR are the main sensors for acquiring wave information. One of the limitations of point measurements is that the acquired information is applicable to a small area, may not be adequate for a large domain. Accurate wave information on fine spatial and temporal resolutions is necessary for navigation, design of coastal/offshore structures, etc. Numerical modelling technique provides an opportunity to obtain the required information on a reasonable resolution both temporal and spatial. Wave information provided by numerical models is crucial to support forecasts and warnings to reduce the risk of accidents and improve the efficiency of marine operations. Therefore, wave prediction has to be done accurately, several days in advance, the full range of sea states from the highest waves in storms to low-amplitude, long-period swells which may have been generated several hundreds of kilometers away.

Wave characteristics along the west and east coast of India are influenced by the three different seasons: pre-monsoon (February – May), southwest monsoon (June – September) and northeast monsoon (October - January). Along the west coast of India, wave heights are usually higher during SW monsoon and low during NE monsoon and pre-monsoon seasons. However, wave heights along the east coast of India are generally high during SW and NE monsoon seasons, and low during pre-monsoon season. In addition to these, tropical storms/cyclones occurring in the Bay of Bengal and in the Arabian Sea will have considerable impact on the wave characteristics along the Indian coast. Storms occur frequently in the Bay of Bengal than in the Arabian Sea. Wave heights above 5 m are usually observed along the coastal regions during tropical cyclones.

During fair weather season, the local winds become dominant due to weakening of global wind systems. Sea breeze and land breeze systems are prevalent along the west coast of India during pre-monsoon season. Wind seas generated due to sea breeze can create a highly dynamic environment in the nearshore regions, and beaches may respond rapidly to the changing wind wave climate. Interaction of local wind seas with pre-existing swells generate complex cross-sea conditions, which makes sea-faring more difficult than a single wave system.

Studies on wave characteristics in the Indian Ocean and coastal regions are primarily based on point measurements of limited duration and satellite measurements. The local wind effects on wind sea generation, interaction of wind seas with pre-existing swells and wave transformation at nearshore and semi-enclosed regions are not studied for the Indian coastal region. In this context, a dedicated effort has been made to understand the above complex phenomena using measurements, modelling and remote sensing. Use of numerical models in wave prediction can significantly improve the understanding of sea states, which are influenced by local wind seas. Fine resolution wave data at the nearshore regions are obtained through numerical simulations using a third generation wave model, which are further utilised to study the wave transformation along open coasts and semi-enclosed areas.

In the present study, numerical models are utilized to predict waves in the Indian Ocean for deep as well as shallow waters. Measured wave parameters at various locations have been used for model validation and detailed analysis. Remotely sensed wave parameters have been used for deep water wave analysis and model comparisons. Wind data obtained from

various sources, namely, in situ, simulated/reanalyzed and remotely sensed (gridded), have been utilized as input to the wave model.

Modelling results have been further applied for operational use in the coastal region. A pilot study for the safety of inland vessels has been carried out for the Mormugao Port region, to demarcate inland vessel's limit (IVL) based on distribution of significant wave heights.

1.3. Objectives

The objectives of the present study are given below:

- i) understanding the wave generation and propagation processes in the select nearshore regions along the Indian coast through measured data.
- ii) validation of wave modelling results of deep and shallow waters using measurements and remote sensing data.
- iii) to study the interaction between pre-existing swells and wind seas generated by coastal winds.
- iv) prediction of wave transformation along the select Indian coasts using high resolution winds such as MM5.

1.4. Area of study

Select locations along the Indian coast have been considered in the present study to understand wave transformation and interaction between local wind seas and pre-existing swells. West and east coasts of India differ in their topographic and bathymetric features and prevailing weather conditions. The east coast of India is characterized by narrow continental shelf width compared to the west coast. The sudden decrease in water depth causes the waves to surge further during extreme events, creating severe coastal hazards (Sanil Kumar et al. 2004c). The Bay of Bengal experiences three different weather conditions—fair weather, southwest monsoon and northeast monsoon. During fair weather season, the sea surface is usually calm and the coastal region is dominated by swells and to a smaller extent by the locally generated waves. Extreme weather events are common during NE monsoon (October–December) season and rare during SW monsoon (June–September) season. The most influencing wind system in the Arabian Sea is SW monsoon,

which has considerable impact along the west coast. During pre-monsoon and NE monsoon seasons, the global winds are generally weak, and the local winds play the major role of controlling the dynamics along the west coast of India.

Figure 1- 3 show the Indian Ocean region and coastal regions considered for the present study. Five locations along the west coast (Dwarka, Mumbai, Ratnagiri, Goa and Kochi) and four locations along the east coast (Nagapattinam, Visakhapatnam, Paradip and Dhamra) have been selected. Mormugao Port region (Figure 1-4) and Dhamra Port region (Figure 1-5) were considered specifically to study wave transformation at semi-enclosed water bodies.

Mormugao Port is situated on the west coast of India. Mormugao bay lies between Mormugao Point ($15^{\circ} 25'N$, $73^{\circ} 47'E$) and Cabo Point. The south of the Mormugao bay is mostly rocky rising upto the tableland of Mormugao Head. The port of Mormugao, protected by a breakwater, lies on the north of Mormugao head. The Cabo point is a prominent headland (55m high).

Dhamra is located on the east coast of India, north of the mouth of the river Dhamra ($20^{\circ} 47.5'N$, $86^{\circ} 57.6'E$). The Port is naturally protected by the river delta (Kanika sands), Gahirmatha landforms and surrounding mangroves, and these morphological features/vegetations dissipate waves propagating from various directions.

Numerical model domains and bathymetry used for the simulations are described in Chapter 3.

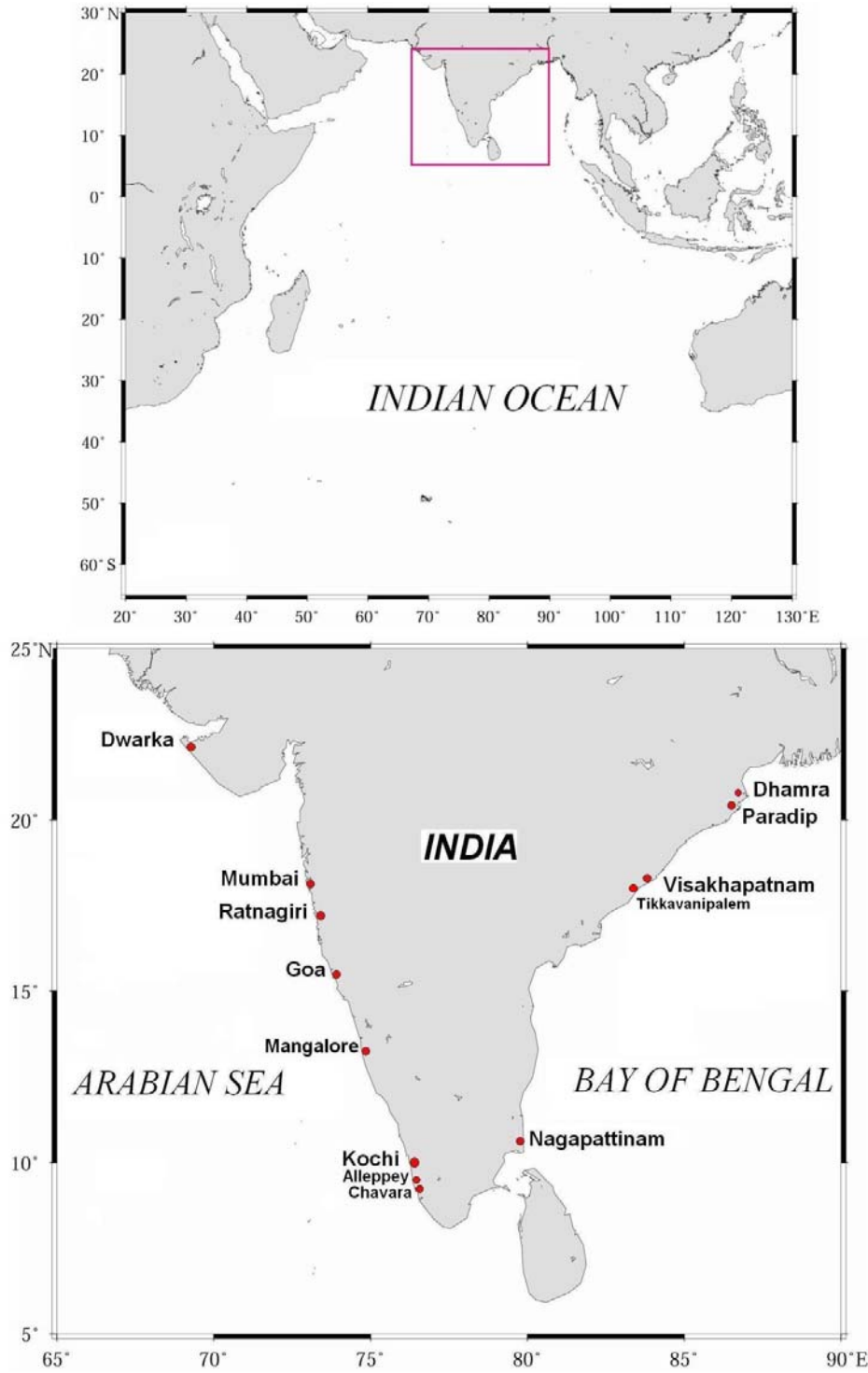


Figure 1- 3. Indian Ocean (top) and Indian coastal regions (bottom) considered for the study.

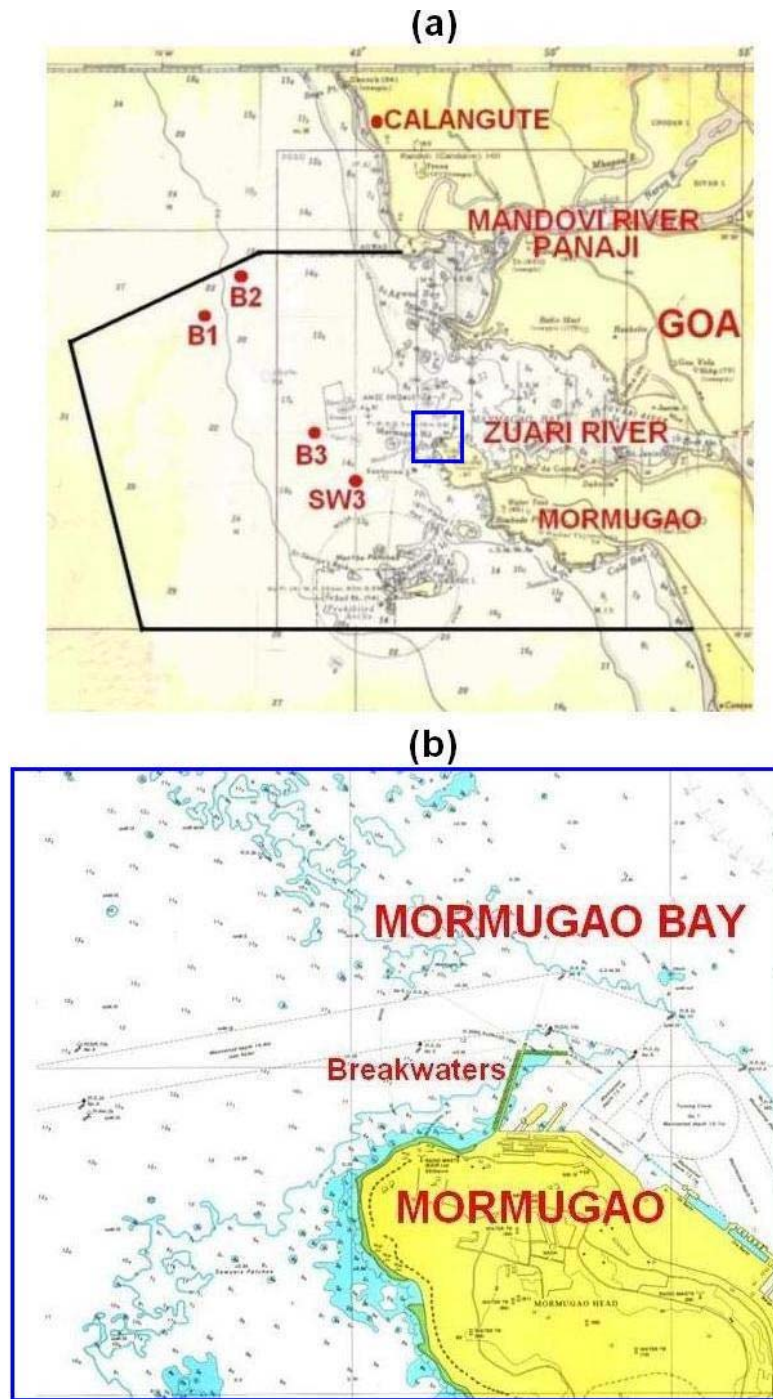


Figure 1-4. (a) Mormugao Port region including the locations of wave rider buoys and moored data buoy off Goa (Mormugao Port limit is marked inside with thick black line) and (b) breakwaters in the Mormugao Port. (taken from NHO Charts 2020 and 2078).

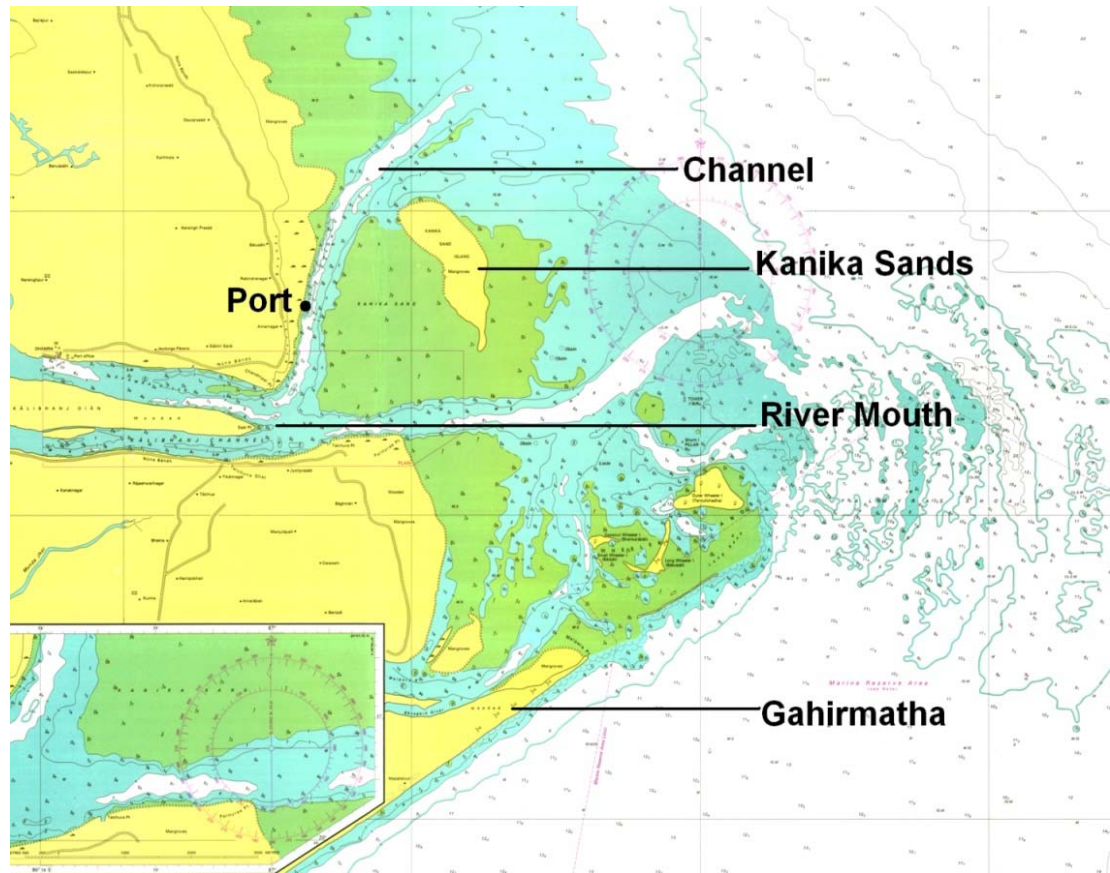


Figure 1-5. Dhamra Port and surrounding areas (taken from NHO Chart 3017).

1.5. Literature review

An extensive literature survey has been carried out to understand the dynamics of ocean waves, their interactions and transformations. As the subject is very vast, only relevant literature related to the specific work has been compiled and presented in the following sections.

1.5.1. Wave generation and growth – historical perspective

The study of ocean wave dynamics has a very long history. Lagrange, Airy, Stokes and Rayleigh, the ‘nineteenth century pioneers of modern theoretical fluid dynamics’ provided details about the properties of surface waves (Phillips, 1977). Jeffreys (1924, 1925) assumed that air flow over the waves causes ‘sheltering’ effect on the lee, so that work could be done by the wind as a result of the pressure difference across the moving wave.

Sverdrup and Munk (1947) postulated that the mechanical energy transferred from winds to water appeared as waves and not as currents. Barber and Ursell (1948) described a method for measuring ocean waves in shallow waters. Valuable contributions of Phillips (1957) and Miles (1957) were added to the theory of wave generation by wind, and this led to rejection of Jeffreys' sheltering hypothesis. Both theories are based on wave generation by resonance: Phillips considered turbulent pressure fluctuations of surface waves, while Miles considered resonant interaction between the wave-induced pressure fluctuations and the free surface waves. Miles' mechanism looks more promising, because it implies exponential growth, and it is of the order of density ratio of air and water.

Miles' theory assumes that the air flow is inviscid, and turbulence does not play a role except in maintaining the shear flow (quasi-laminar approach). However, this approach oversimplifies the real problem. Early field experiments and laboratory studies by researchers (e.g., Dobson, 1971; Snyder, 1974; Snyder et al, 1981; Hasselmann and Bosenberg, 1991) show that the rates of energy transfer from wind to waves are larger than those predicted by Miles, especially for low-frequency waves. There are several limitations for the quasi-laminar approach; turbulence was not properly modelled and it ignored severe nonlinearities and wave-mean flow interaction. Wave-mean flow interaction is expected to be important at the height where the wind speed matches the phase speed of the surface waves (the so-called critical height). The advent of numerical modelling of the turbulent boundary layer flow over a moving sea surface resolved the issues associated with the turbulence for some extent. Further approaches (e.g., Al-Zanaidi and Hui, 1984; Jacobs, 1987 and Chalikov and Makin, 1991) considered the direct effects of small-scale turbulence on wave growth. Mixing length modelling or turbulent energy closure is then assumed to calculate the turbulent Reynolds stresses. However, the results are not very different from the one obtained in the quasi-laminar theory. Therefore, small-scale eddies and nonlinearities in wave steepness have only a small direct effect on wave growth. The efforts made by Fabrikant (1976) and Janssen (1982) on the theory of interaction of wind and waves indicates that at each particular time the wave growth follows Miles' theory and the results have been confirmed by observations. Combination of observations from field campaigns in the 1970's and the theoretical work on critical layer mechanism which started in the 1950's resulted in parameterizations of the wind-input source function. This provided good results in operational wave models.

Mixing length modelling assumes that the momentum transfer caused by turbulence is the fastest process in the fluid. This is not justified for low-frequency waves which interact with large eddy whose eddy-turnover time may become larger than the period of the waves. Nikolayeva and Tsimring (1986) considered the effect of gustiness on wave growth, and found a considerable enhancement of energy transfer due to large-scale turbulence, especially for long waves with a phase speed comparable to the wind speed at 10 m height. Belcher and Hunt (1993) have pointed out that mixing length modelling is even inadequate for slowly propagating waves. They argue that far away from the water surface turbulence is slow with respect to the waves so that again large eddies do not have sufficient time to transport momentum. This approach has been further developed by Mastenbroek (1996) in the context of a second-order closure model for air turbulence, confirming the ideas of rapid distortion. Following the rapid-distortion ideas, Janssen (2004) argued that the large eddies are too slow to transport a significant amount of momentum during one wave period.

The most direct evidence for the dependence of the air flow on the sea waves comes from the observed dependence of the drag coefficient on the so-called wave age (c_p/u_* , where c_p is the phase speed of the peak of the spectrum and u_* the friction velocity). Measurements by, for example, Donelan (1982), Maat et al (1991), Smith et al. (1992), Drennan et al. (1999) and Oost et al. (2002) indicate that the drag coefficient depends on the sea state through the wave age. For a fixed wind speed at 10 m height, the drag coefficient of air flow over young wind sea is 50% larger than the drag coefficient over old wind sea (Donelan, 1982). Including the effects of small scale turbulence, Jenkins (1992) observed similar results of the drag coefficient as obtained in the quasi-linear theory. Komen et al (1994) found that quasi-linear theory of wind wave generation gives a better description of momentum transfer than the usual theory of wave growth since quasi-linear theory gives a drag coefficient that describes the sea state dependence on the drag.

Parameterization of the roughness length in terms of wave-induced stress shows a fair agreement with observed roughness (Janssen, 1992). Short waves are the fastest growing waves; the wave-induced stress is to a large extent determined by the spectrum of the high-frequency waves (see, e.g. Janssen, 1989; Makin et al., 1995). Using wavelet analysis, Donelan et al. (1999) found that wavenumber spectrum of the short waves depends in a sensitive manner on wave age: ‘young’ wind sea shows much steeper short waves than ‘old’ wind sea. Sullivan et al. (2000) studied the growth of waves by wind in the context of

an eddy-resolving numerical model. He found a rapid fall-off of the wave-induced stress at the critical height, as expected from the Miles mechanism. The growing waves act as a rectifier, therefore gustiness may have a considerable impact on wave growth (Abdalla and Cavaleri, 2002). Furthermore, Hristov et al. (2003) identified direct evidence of the existence and relevance of the critical layer mechanism from in-situ observations obtained from FLIP (FLoating Instrument Platform). For long waves, a positive fluctuation in wind speed will result in enhanced wave growth but, a negative fluctuation will not give rise to reduced growth (WISE Group, 2007).

1.5.2. Wave energy spectrum

The concept of wave spectrum was first introduced to wind wave studies around 1950. Over the following decades, Fourier spectrum was the standard procedure used to analyse and predict wind waves. Notably, Barber and Ursell (1948) carried out the first measurement and analysis of wave spectra. Pierson and Marks (1952) introduced power spectrum analysis in wave data analysis. Later, the methods introduced by Pierson et al. (1955) led to the advancement of understanding wave dynamics. Wavelet analysis evolved as an effective alternative to the standard Fourier analysis (Combes et al., 1989). Further, with the development of Fast Fourier Transform (FFT), spectrum analysis becomes routine in time series wave data analysis (Liu, 2000).

The directional wave energy spectra provide a complete description of the wave energy distribution over spectral frequencies f and direction θ . The energy-density spectra can be written in the form of $E(f, \theta) = E(f)D(f, \theta)$, where, $E(f)$ represents the frequency spectrum which is assumed as a function of significant wave height (H_s) and the peak frequency (f_p), while $D(f, \theta)$ represents the directional spectrum which is assumed by the mean wave direction (θ) and directional spreading parameter (s).

As sea state consists of local wind-generated waves and swells of distant storms, the wave energy spectra often show two or more spectral peaks corresponding to different generation sources. Depending on sea states and measurement sites, the occurrence of double-peaked spectra could be even higher. Guedes Soares (1984) proposed the ratio of peak frequencies of the two components as spectral parameters to describe the relation of the two wave systems. Relatively close double peaks (looks as if single-peaked) indicate combination of sea state with two wave systems coming from the same or different directions (Guedes Soares, 1991). According to Torsethaugen and Haver (2004), single-peakedness occurs

when spectral peak period (T_{pf}) for fully developed sea equals peak wave period (T_p). The sea dominance occurs when $T_p < T_{pf}$, where the spectral peak is in the high frequency region, and double or multiple peaks present during such conditions. The swell dominance occurs when $T_p > T_{pf}$, where the spectral peak is in the low-frequency region.

Separation of sea and swell parameters from the spectra is essential to understand the dynamics associated with each system. Identification and separation of the wave energies of wind sea and swell from the measured spectra allow us to have a more realistic description of the sea state, which is of great importance to offshore structural design, safety of marine operation and for the study of wind wave dynamics (Wang and Hwang, 2001). Algorithms are developed to separate wind sea and swell components from wave spectra. The partitioning methods primarily involve separating the wave spectra into two frequency bands: a low-frequency interval (swell component) and a high-frequency interval (wind sea component). Most methods for the automatic identification and separation of wave components of wind sea and swell rely on the determination of a separation frequency f_s for a given wave spectrum. Wang and Hwang (2001) used a separation frequency, f_s based on wave steepness to distinguish between wind seas and swells. Wave components with frequencies greater than f_s are generated by local winds and those with frequencies less than f_s are from distant swells. Earle (1984) proposes an empirical relation between the separation frequency and the local wind speed U based on the Pierson-Moskovitz (PM) spectral model (Pierson and Moskowitz, 1964). The algorithm introduced by Gerling (1992) takes into account identification and grouping of component wave systems from spatially and temporally distributed observations of directional wave spectra. Using wind and wave directional data, a directional spectra partitioning scheme has been developed for identifying wind sea and tracking storm sources (Gerling, 1992; Kline and Hanson, 1995; Hanson, 1996; Hanson and Phillips, 2001).

Violante-Carvalho et al. (2004) studied the wind sea and swell characteristics at Campos Basin, South Atlantic by calculating the sea-swell parameters from measured spectral data. Using an empirically determined width of the confidence intervals of the spectral data, a procedure is developed by Rodriguez and Guedes Soares (1999) to differentiate legitimate energy peaks of wind sea and swell from the spectral irregularities caused by the artifacts of random processes. Portilla et al. (2009) discussed various techniques and methods for partitioning and identifying wind sea and swell. Gilhousen and Hervey (2001) provided techniques to improve accuracy of the estimates of swell from moored buoys. This method

determines a separation frequency by assuming that wind seas are steeper than swells and that maximum steepness, or ratio of wave height to length, occurs in the wave spectrum near the peak of wind sea energy. This method has been used by National Data Buoy Centre (NDBC), NOAA, USA.

1.5.3. Remote sensing

Wind and wave data obtained from remotely sensed sources such as scatterometer and altimeter are widely used to understand wind and wave patterns around the globe. Remote sensing data are widely used in operational oceanography by assimilating them with third generation models.

Surface waves are measured by active microwave sensors by transmitting electromagnetic energy. Highly sophisticated signal analysis has made it possible to obtain information on the ocean waves by studying the reflected signal. The first ocean satellite SEASAT demonstrated in 1978 that wave heights could be accurately measured with a radar altimeter and that a SAR (Synthetic Aperture Radar) was capable of imaging ocean waves. Unfortunately, SEASAT failed after three months, and further satellite wave measurements were not made until the radar altimeter aboard GEOSAT was put into orbit in 1985. After the short parenthesis of GEOSAT operated till 1989, satellite data began flowing in 1991 with the launch of the first European Remote Sensing Satellite ERS-1, followed by Topex/Poseidon in 1992 and in 1995 by ERS-2. These satellites have onboard an altimeter (ERS 1 & 2 and Topex) and a scatterometer (ERS 1 & 2). The altimeter provides wind speed and wave height at 7 km intervals (once a second) along the ground track of the satellite. The scatterometer provides wind data, all along the width of the swath, a few hundreds of kilometers. ERS 1 and 2 have been following an orbit with a return period of 30 days; however, Topex has been following an orbit with 10 days period. Since 1999, wind data from QuikSCAT and since 2002, wave data from Jason-1 are available.

The SEASAT altimeter showed a good match when compared with buoy wave heights (Graber et al, 1996). Earlier studies for the ERS-1 altimeter (Goodberlet et al, 1992 and Gunther et al, 1993) also showed match for wave heights upto 4 m, although high waves tend to be underestimated by the altimeter relative to the buoy measurements. Mastenbroek et al (1994) reached a similar conclusion from a comparison of ERS-1 data with North Sea observations. The accuracy of altimeter wave height measurements is confirmed also by the global inter-comparison of ERS-1 altimeter and WAM model wave

heights for the month of July 1992 (Komen et al., 1994). The altimeters in Topex and ERS 1 & 2 provide accuracy of 2m/s in wind speed and 10% or 50 cm (whichever is better) in wave height (Duchossois, 1991; Fu et al., 1994). The wind speeds derived from the altimeter are not reliable at very low wind speeds, the threshold speed being 2 m/s. The retrieval algorithm also loses its reliability in the very high value range, above 20 m/s, due to physics involved in the sea surface processes.

The SeaWinds scatterometer onboard QuikSCAT gives instantaneous wind vectors along a wide swath (1800 km) with a spatial resolution of 25 km and two passes per day (ascending and descending) (Ebuchi et al., 2002). The accuracy of wind speed is 2 m/s between 3 and 20 m/s (approximately 10%) and that of wind direction is 20°. The gridded product of QuikSCAT winds were derived by IFREMER and it is available globally in every 0.5° x 0.5° (C2-MUT-W-03-IF, 2002). Gille et al. (2003) used QuikSCAT data to study the characteristics of sea breeze and land breeze systems present in most of the world's coastlines. Aparna et al. (2005) studied the seaward extension of the sea breeze along the southwest coast of India utilizing QuikSCAT winds. Satheesan et al. (2007) analysed the QuikSCAT winds by comparing with buoy winds in the Indian Ocean.

Jason-1 is relatively a small satellite developed by NASA and CNES for measuring oceanographic and meteorological parameters. It provides significant wave heights and wind speeds along the satellite ground tracks over 6-7 km with repeat cycle of 7 days. Gridded product of Jason-1 provides significant wave heights for every 1° x 1° resolution in alternate 3 and 4 days (Quilfen et al, 2004). The calibration of Jason-1 data (wind and wave) has been carried out by Bonnefond et al. (2003) and Chambers et al. (2003). Ardhuin et al. (2007) validated these data with buoy observations. Bhatt et al. (2005) used Jason-1 significant wave heights to assimilate in a third generation wave model.

The altimeter and scatterometer data may not be accurate close to the coast because of the interference with the land. Besides, when the satellite moves towards offshore, and entered in the marine area, it requires certain time to work properly again. This implies that reliable wind speeds are not available upto 25-30 km off the coasts (Cavaleri and Selavo, 2006).

1.5.4. First, second and third generation models

Interest in wave prediction grew during the Second World War II because of the practical need for knowledge of the sea state during landing operations. At first, Sverdrup and Munk (1947) introduced a parametrical description of the sea state and empirical wind sea and

swell laws for the operational wave predictions. Gelci et al., (1957) introduced the concept of the spectral transport equation and he used a purely empirical expression for the net source function governing the rate of change of the wave spectrum. Based on the wave generation theories provided by Philips (1957) and Miles (1957), Hasselmann (1962) introduced the source functions for the nonlinear transfer. The general expression for the source function consists of three terms representing the input from the wind, the nonlinear transfer and the dissipation by white-capping or bottom friction.

A numerical spectral wave model calculates the evolution of the wave energy according to physical laws governing the change of wave energy. Several first and second generation numerical models were developed in the last few decades. Subsequently, third generation wave models were developed and at present, a few of them are widely used for the operational wave forecasting. Theoretical explanations about numerical wave modelling and a third generation wave model WAM are described in Komen et al. (1994).

1.5.4.1. First generation models

The first empirical wave model was developed by Sverdrup and Munk (1947) and introduced a parametric description of the sea state. Subsequently, PNJ-model was developed for estimating wave conditions created by distant storm (Pierson et al., 1955). Darbyshire (1961) made significant improvements in the PNJ-model and used it to predict waves over the North Atlantic. It was assumed that the sea state was fully developed after 12 hours and 200 nm of constant wind. However, the model proposed by Wilson (1955) was considered as ideal, and further used by several researchers (e.g., Bretshneider, 1963 and Barnett and Wilkerson, 1967). A directional de-coupled model was developed by Seymour (1977), in which a stationary homogeneous wind field is considered over a deep water basin with an arbitrary geometry of the coastline.

The first generation models accounted only wave energy growth and dissipation. At that time, very little was known about nonlinear interactions and energy loss due to whitecapping, and hence these were not taken into account in the first generation models. Later, it became clear that interactions between waves of different frequencies were important in determining the distribution of wave energy in the spectrum. These non-linear interactions are very difficult and expensive to compute explicitly, and parameterizations were developed to account for the effect.

1.5.4.2. Second generation models

Wave models using a parameterization of the non-linear interactions are known as 'second generation'. In second generation models, the sea surface is defined as the sum of a large number of individual wave components, each wave propagating with constant frequency according to the linear wave theory. The path of wave components is calculated by the conventional methods. After leaving the origin, the wave component interacts with the other wave components. Thus, the energy gained or released in the process can be evaluated till it reaches the forecast point at regular intervals.

Typically, there are two types of models in the second generation; coupled hybrid and coupled discrete. In coupled hybrid models the wind sea spectrum, which is strongly controlled by the nonlinear interactions, is assumed to adjust rapidly to a universal quasi-equilibrium form in which only a single scale parameter – normally the wind sea energy – or at the most a second frequency scale parameter need to be predicted as slowly varying parameters. The swell, which is not affected by nonlinear interactions, is then treated as a superposition of independent components in the same way as in a first generation model. Coupled discrete models retain the traditional discrete spectral representation, but have a parameterization of the nonlinear transfer with limited validity, so that the potential advantage of a more flexible representation of the wind sea spectrum and a uniform representation of the swell – wind sea transition regime cannot be properly exploited. Mandal (1985) used a deep water hybrid point model DOLPHIN developed by Holthuijsen and De Boer (1988), which is a combination of parametric wind-sea and spectrally treated swells. It is based on the directionally decoupled energy distribution of wind generated waves.

Results from many of the operational first and second generation models were inter-compared in the SWAMP (1985) study. Although the first and second generation wave models can be calibrated to give reasonable results in most wind situations, the inter-comparison study identified a number of shortcomings, particularly in extreme wind and wave situations for which reliable wave forecasts are most important. The differences between the models were most pronounced when the models were driven by identical wind fields from a hurricane. The models gave maximum significant wave heights in the range 8 to 25 m.

1.5.4.3. *Third generation models*

Further developments led to an approximation for the non-linear energy transfer, which consider the four most important interacting waves at each frequency out of the infinite number of interactions theoretically possible. This approximation is more expensive to compute than the parameterization of a second-generation model but, unlike a second-generation model, the wave spectrum is not forced to take a particular form for growing wind-sea, and is free to evolve according to the physical equations. Such a wave model is called 'third generation'. The major limitations of the first and second generation models are:

- first generation models do not have an explicit S_{nl} term. Non-linear energy transfers are implicitly expressed through the S_{in} and S_{ds} terms, where S_{nl} , S_{in} and S_{ds} are the source terms representing energy transfer due to non-linear interactions, energy input from wind and energy loss due to dissipation, respectively.
- second generation models handle the S_{nl} term by parametric methods: for example, by applying a reference spectrum (say, JONSWAP or Pierson-Moskowitz spectrum) to reorganize the energy (after wave growth and dissipation) over the frequencies.

As a consequence of the variable results from the SWAMP study, and with the advent of more powerful computers, scientists began to develop new, third generation wave models which explicitly calculate each mechanism identified in wave evolution. The main difference between the second and third generation wave models is that in the latter case, the wave energy-balance equation is solved without constraints on the shape of the wave spectrum. This is achieved by accurately calculating the S_{nl} term. Resio et al. (1991) derived a new method for the exact computation of this term. Hasselmann and Hasselmann (1985) introduced Discrete Interaction Approximation (DIA) in wave modelling. The efficient computation of the non-linear source term together with more powerful computers made it possible to develop third generation spectral wave prediction models (WAMDI Group, 1988). The operational wave models, such as WAM (WAMDI Group, 1988 and Komen et al., 1994), SWAN (Booij et al., 1999) and WAVEWATCH III (Tolman, 1999) are third generation models.

Third generation wave models are similar in structure, representing the state-of-the-art knowledge of the physics of the wave evolution. For the WAM model, the wind input term, S_{in} , for the initial formulation was adopted from Snyder et al. (1981) with a u_* (friction

velocity) scaling instead of U_5 (wind speed at 5 m). This has been superseded by new quasi-linear formulations by Janssen (1992) and Komen et al. (1994), which include the effect of growing waves on the mean flow. The dissipation source function, S_{ds} , corresponds to the form proposed by Komen et al. (1984), in which the dissipation has been tuned to reproduce the observed fetch-limited wave growth and to eventually generate the fully developed Pierson-Moskowitz spectrum. The non-linear wave interactions, S_{nl} , are calculated using the discrete interaction approximation of Hasselmann et al. (1985). The model can be used both as deep water and shallow water model (WAMDI Group, 1988). A comprehensive description of the model, its physical basis, and formulation and various applications are given in Komen et al. (1994). Other models may differ in the propagation schemes used, in the method for calculating the nonlinear source term, S_{nl} , and in the manner in which they deal with shallow water effects and the influence of ocean currents on wave evolution. In general, the governing equation (so called energy balance equation) applied in the third generation model is,

$$\frac{\partial F}{\partial t} + \mathbf{c}_g \cdot \nabla F = S_{in} + S_{nl} + S_{dis} \quad (1.8)$$

where, the left hand side terms represent the time derivative and the kinematics of the field, and the right hand ones the physical processes at work for its evolution. $\partial/\partial t$ is the derivative with respect to time, \mathbf{c}_g is the group speed and ∇F represents the spatial gradient of the field.

Vladder (2001) improved the parameterization of nonlinear quadruplet wave-wave interactions for application in operational wave prediction models. Further improvements have been carried out to obtain a fast and accurate method for computing the nonlinear quadruplet wave-wave interactions in deep and shallow water. For reaching closer values of non-linear transfer, Tolman et al. (2005) developed a neural network parameterization called Neural Network Integration Approximation (NINA), which estimates nonlinear interactions as a function of frequency and direction from the corresponding spectrum in deep water. It is implemented in WAVEWATCH III model. Neural networks can be incorporated in numerical wave modelling for solving complex nonlinear functions in an efficient way (Mandal and Prabaharan, 2010).

The third generation models are widely used for operational wave forecasting. European Centre for Medium-Range Weather Forecasts (ECMWF) extensively use WAM model for

operational wave forecasting. Prasad Kumar and Stone (2007) used the third generation model, WAM to simulate the generation and propagation of typhoon waves in Korean seas. Kurian et al. (2009), Vethamony et al (2009) used third generation wave model, MIKE 21 SW, developed by Danish Hydraulic Institute (DHI), Denmark to simulate waves around the Indian Ocean and west coast of India. Aboobacker et al., (2009) used this model to simulate waves off Paradip, east coast of India.

1.5.5. Impact of sea breeze on nearshore waves

The sea breeze circulation system - a common mesoscale meteorological phenomenon - has a profound effect on the meteorology and oceanography of coastal areas (Simpson, 1994). It flows perpendicular to the coastline and drives a density current that moves cool moist marine air over the land. The sea breeze is at its maximum in the late afternoon. Relatively low speed land breeze starts blowing towards the sea in the night.

A few studies have been carried out on wave characteristics due to sea breeze. For example, the coastal region of Sydney, Australia, was studied by Linacre and Hobbs (1977), Short and Trenaman (1992) and Masselink and Pattiaratchi (1998). They observed that the sea breeze is most prevalent between 12 and 21 h (local time) during the summer season (October – April), and typically produces a wave with 1 – 1.5 m height and periods ranging between 6 and 9 s. Masselink and Pattiaratchi (1998) pointed out that, following the onset of the sea breeze, the addition of locally generated wind waves to background swell resulted in an increase in wave height and a decrease in wave period. Verhagen and Savov (1999) studied wave growth due to sea breeze in Cartagena (Colombia) region, and estimated the duration of wave action based on that of the sea breeze.

Sea breeze induces changes to the incident wave field that may significantly affect beach morphology and processes. Sonu et al. (1973) observed increase in nearshore wave height, decrease in wave period and change in wave angle depending on the direction of the sea breeze after the onset of the sea breeze, typically late morning or early afternoon. As a consequence, wave energy, current velocities, suspended sediment concentrations and sediment transport rates increase dramatically following the commencement of sea breeze (Pattiaratchi et al., 1997).

1.5.6. Wave transformation

Wind-generated waves are identified as the major driving force for near-shore circulation and sediment transport in the surf zone and inner continental shelf (Wright *et al.*, 1991). When the waves approach the shallow depths, the group velocity starts to reduce. This generally leads to turning of the wave direction (refraction) and shortening of wavelength (shoaling), which may result in increase or decrease in wave height. The most important physical processes, which affect the waves in shallow waters are dissipation due to bottom friction (e.g. Shemdin *et al.*, 1980), bottom induced wave breaking (e.g. Battjes and Janssen, 1978) and triad wave-wave interactions (e.g. Madsen and Sorensen, 1993).

As waves shoal in coastal waters, wave energy spectra evolve due to refraction, nonlinear energy transfers to higher and lower frequencies (Freilich and Guza 1984; Freilich *et al.*, 1990), and energy dissipation caused by wave breaking and bottom friction (Thornton and Guza, 1983; Sheremet and Stone, 2003). Smith and Vincent (2002) found that in the inner surf zone, wave spectra evolve to a similar, single-peaked shape, regardless of the complexity of shape outside the surf zone. It is postulated that spectral shape evolves from the strong nonlinear interactions in the surf zone.

Extensive observations in the Joint North Sea Wave Project (JONSWAP) revealed that swell attenuates in shallow water by bottom friction and the relative reduction in wave height is more pronounced for increasing near-bottom velocities (Hasselmann *et al.*, 1973). Ardhuin *et al.* (2003) studied attenuation and directional transformation of waves in swell dominated conditions across North Carolina continental shelf during the 1999 Shoaling Waves Experiment (SHOWEX). They observed strong attenuation of large swells across the wide and shallow shelf, with typical wave height reductions of factor 2, and relatively weak variations for small swells with $H_s < 1.0$ m offshore. Strong decay of energetic swell in the absence of local winds suggests that dissipation of wave energy by bottom friction is the primary attenuation mechanism. Among other possible swell dissipation mechanisms, percolation was estimated to be much smaller than bottom friction for fine to medium sand and significant only for coarser sediments, while bottom elasticity is only important over sediments composed of mud or decomposed organic matter (Shemdin *et al.* 1980). In addition to dissipative processes, backscattering of waves by the bottom topography may cause attenuation of waves toward the shore (Long 1973), but the estimated wave decay over actual bathymetry is extremely weak (Richter *et al.*, 1976; Ardhuin and Herbers

2002). However, forward scattering of waves can cause significant broadening of wave directional spectra (Ardhuin and Herbers, 2002).

Models for the wave transformation are important to predict nearshore circulation and sediment transport. In addition to the well understood linear processes of shoaling and refraction, the wave transformation is affected by nonlinear interactions and wave breaking (Herbers et al., 2003). These interactions not only broaden the frequency spectrum in shallow water, but also phase couple the spectral components, causing characteristic steepening and pitching forward of near-breaking wave crests (e.g., Freilich and Guza, 1984; Elgar and Guza, 1985). This nonlinear evolution is described well by depth integrated Boussinesq equations for weakly nonlinear, weakly dispersive waves in varying depth (Peregrine, 1967). Most models for the breaking of random waves are based on the analogy of individual wave crests with turbulent bores (Battjes and Janssen, 1978; Thornton and Guza, 1983). Estimates of nonlinear energy transfers in the surf zone based on bi-spectral analysis of near-bottom pressure fluctuations confirm the dominant role of triad interactions in the spectral energy balance (Herbers et al., 2000).

1.6. Studies along the Indian Ocean region

Studies on ocean surface waves carried out in the Indian Ocean waters and briefly given below: Sundara Raman et al. (1974) studied the distribution of wave characteristics in the coastal waters off Mangalore, southwest coast of India. They found that the relative frequency of occurrence of long period waves increases from April to November. Baba et al. (1983) studied wave refraction in relation to beach erosion along the Kerala coast, southwest coast of India. Kurian et al. (1985) studied wave transformation off Alleppey, southwest coast of India using a refraction model developed by Dobson (1967) and, subsequently modified by Coleman and Wright (1971) to accommodate bottom frictional attenuation. Wave damping and attenuation due to mud banks along the Kerala coast have been well studied by Mac Pherson and Kurup (1981), Mathew et al. (1995) and Jiang and Mehta (1996). Kurian and Baba (1987) conducted a detailed study of wave attenuation due to bottom friction at select locations across the southwest Indian continental shelf. Chandramohan et al. (1991) used ship observed data to study wave statistics around the Indian coast. Swain et al. (1993) studied shallow water wave characteristics off Cochin during the southwest monsoon of 1986. Directional spreading of waves in shallow waters have been studied by Sanil Kumar et al. (1999). They found that in shallow water, wave

directional spreading is narrow at the peak frequency and wide towards lower and higher frequencies. Shahul Hameed et al. (2007) studied seasonal and annual variations in wave parameters off Chavara coast, southwest coast of India, based on continuous measurements of 2 years.

Harish and Baba (1986) and Rao and Baba (1996) studied spectral characteristics of waves along the southwest coast of India and observed that the spectra are generally multi-peaked. Vethamony and Sastry (1986) studied the characteristics of multi-peaked spectra of ocean surface waves. Baba et al. (1989) also analysed the wave spectra off Cochin, southwest coast of India and studied the swell characteristics. Rao and Baba (1996) studied the wind sea and swell characteristics along the southwest coast of India and identified that wind sea energy was dominant over swell energy during pre-monsoon period. Sanil Kumar et al. (2000) studied the wave characteristics along the west coast of India during southwest monsoon and observed that swells are predominant during southwest monsoon season. Sanil Kumar et al. (2001) separated seas and swells from directional wave data collected off Tikkavanipalem, east coast of India and estimated longshore currents and longshore sediment transport rate. Sanil Kumar et al. (2002) studied sea and swell characteristics off Nagapattinam coast, east coast of India based on one year continuous directional wave measurements. Sanil Kumar et al. (2003a) studied multi-peakedness and groupiness of shallow water waves along the Indian coast. Sea and swell dominated double peaked spectra were present for different periods at various locations. Sanil Kumar and Anand (2004a) used first and second order Fourier coefficients to estimate variations in wave direction at four locations in the west and east coast of India. Considering directional distribution of waves at three locations along the Indian coast and 18 years of ship reported data, Sanil Kumar and Deo (2004b) estimated design wave parameters. Sanil Kumar and Ashok Kumar (2008) analysed spectral characteristics of high shallow water waves (significant wave heights above 2 m) and derived an empirical equation relating the JONSWAP parameters with significant wave height, peak wave period and mean wave period. Aboobacker et al. (2005 and 2009) studied spectral characteristics off Paradip during monsoons and extreme events. Vethamony et al., (2009) analysed the spectra measured off Goa during pre-monsoon season.

Numerical simulations have been carried out in the Indian Ocean to study the wave characteristics during various seasons (e.g., Aboobacker et al., 2009; Vethamony et al., 2009; Rajkumar et al., 2009; Kurian et al., 2009). Abhijit Sarkar et al. (1997) simulated

waves in the north Indian Ocean and compared predicted wave heights with altimeter measurements. Sudheesh et al. (2004) assessed wave modelling results with deep water buoy measurements and altimeter data during southwest monsoon. Vethamony et al. (2006) simulated waves in the north Indian Ocean using MSMR (Multi-channel Scanning Microwave Radiometer) analysed winds.

Prasad Kumar et al. (2000) analysed extreme wave conditions over the Bay of Bengal during severe cyclone utilizing numerical simulations. They used a second generation wave model (Resio model) and a third generation wave model (WAM) to simulate state of the sea for an exceptionally severe cyclone which occurred over the Bay of Bengal during November 1977. Sanil Kumar et al. (2003b) studied the wind and wave characteristics during cyclones (1960 – 1996), which crossed Nagapattinam coast, by estimating the wind speeds and wave heights using various techniques. Based on measured wave energy spectra, Sanil Kumar et al. (2004c) demonstrated wave characteristics along the Visakhapatnam coast, east coast of India during an extreme event. They identified that the spectra were single-peaked during the storm event and percentage occurrence of double-peaked spectra were higher during low sea states.

The sea state of the Indian Ocean is significantly modified by swells, and it has considerable implications on the coastal regions of India (Raj Kumar et al., 2009). However, role of local winds on wind sea generation along the Indian coast is not well understood. Only a few studies has been carried out on this aspect. Neetu et al. (2006) studied the impact of sea breeze on the wind seas off Goa, west coast of India. They identified that large scale winds are weak during pre-monsoon periods and hence the sea breeze has an impact on the diurnal cycle of the sea state along the west coast of India. Vethamony et al. (2009) also studied the characteristics of the waves off Goa during pre-monsoon season, when the sea-breeze dominates over global winds. They found that the diurnal pattern is due to the co-existence of locally generated wind seas and pre-existing swells. An in depth study on the influence of sea breeze on the pre-existing swells from the Indian Ocean has been carried out as part of the present work, and the results are discussed in the following chapters.
